1.D.1 *Nuclear Physics* **A186** (1972) 365—378; © *North-Holland Publishing Co., Amsterdam*

SHELL-MODEL CALCULATIONS FOR MASSES 27, 28 AND 29: ELECTROMAGNETIC TRANSITION RATES AND MULTIPOLE MOMENTS

M. J. A. DE VOIGT, P. W. M. GLAUDEMANS and J. DE BOER
Fysisch Laboratorium, Rijksuniversiteit, Utrecht, The Netherlands

and

B. H. WILDENTHAL
Michigan State University, East Lansing, Michigan 48823

Received 17 February 1972

Abstract: Electromagnetic transition probabilities, multipole moments and log *ft* values have been calculated from many-particle shell-model wave functions in a truncated $1d_{\frac{5}{2}}\,2s_{\frac{1}{2}}\,1d_{\frac{3}{2}}$ configuration space, with a maximum of four holes in the $1d_{\frac{5}{2}}$ subshell. The electric quadrupole transition strengths and moments are reproduced very well in a least-squares fit to 74 experimental data with one parameter, for the isoscalar effective charge, yielding the values $e_p = 1.6\,e$ and $e_n = 0.6\,e$. The results for magnetic dipole transition strengths and moments follow from adjusting two effective reduced single-particle matrix elements in separate least-squares fits to 17 experimental data in $A = 27$ nuclei and 21 data in $A = 29$ nuclei. The average absolute deviations between theory and experiment for E2 and M1 transition strengths are 3.0 and 0.05 W.u., while the average measured strengths are 7.7 and 0.08 W.u., respectively. Transitions from excited states above $E_x = 4.8$ MeV in ^{27}Al and from some low-lying states in ^{27}Al and ^{28}Si are poorly reproduced by the present model. Calculated strengths of transitions from analogue states are given. Previous conclusions about the single-particle character of M1 transitions and the collective behaviour of E2 transitions are confirmed. The experimental data of seven $A = 27$–29 nuclei are well reproduced in one general treatment with an appreciably lower number of free parameters than are required to obtain comparable results in collective model calculations.

1. Introduction

A possible rotational-like structure of the nuclei around mass 28 has been discussed by several authors [1–6]). Since many-particle shell-model calculations in the mass region $A = 30$–34 have met with considerable success [7, 8]), it was thought worthwhile to extend these calculations to the slightly lighter $A = 27$–29 nuclei. The electromagnetic properties are reported here. The excitation energies and spectroscopic factors are discussed in another paper [9]). The electric quadrupole moments of ^{27}Al and ^{28}Si as found in a previous calculation have already been published [10]). Similar calculations for $A = 23$–27 nuclei of which some have an established deformed character are in progress [11]).

These calculations are feasible since a wealth of experimental information on $A = 27$–29 nuclei became available recently (see table 1). The wave functions have been calculated [9]) with the Oak Ridge-Rochester shell-model computer programs [12]). The configuration space is given by: $(1s)^4(1p)^{12}(1d_{\frac{5}{2}})^{n_1}(2s_{\frac{1}{2}})^{n_2}(1d_{\frac{3}{2}})^{n_3}$ with $n_1+n_2+n_3$

$= A-16$; $n_1 \geqq 8$ for $A = 27$ and 28, whereas for $A = 29$ the $n_1 \geqq 9$ and the $n_1 = 8$, $n_2 = 4$, $n_3 = 1$ configurations have been taken along. The modified surface delta interaction [13]) has been used as an effective two-body interaction. The calculations have been performed for even-parity levels in $A = 27$ and 29, $T = \frac{1}{2}$ and $\frac{3}{2}$ and $A = 28$, $T = 0$.

A sensitive test of wave functions is the comparison of calculated electromagnetic transition rates and multipole moments with experimental data.

2. The least-squares fitting procedure

The theory underlying the use of effective electromagnetic operators and the fitting procedure by which the empirical effective values are obtained have already been discussed in detail in ref. [8]).

In order to save computer time, contributions from the wave functions have been taken into account only if $a_n b_m \geqq 0.0005$, where a_n and b_m denote the amplitudes of initial and final state wave function components, respectively. Even for very weak transitions the contributions of weaker components were found to amount to only a few percent. Some properties of the wave functions are illustrated in fig. 1 as a function of the truncation amplitude. Examples of the effect of amplitude truncation on some calculated transition strengths and one dipole moment are given in fig. 2. These two figures clearly demonstrate that a large fraction ($\approx 50\,\%$) of the total number of components do not contribute significantly to the transition rates and to the norm ($\sum a_n^2$) of the complete wave functions.

The relative signs of the experimental transition amplitudes, which are needed in

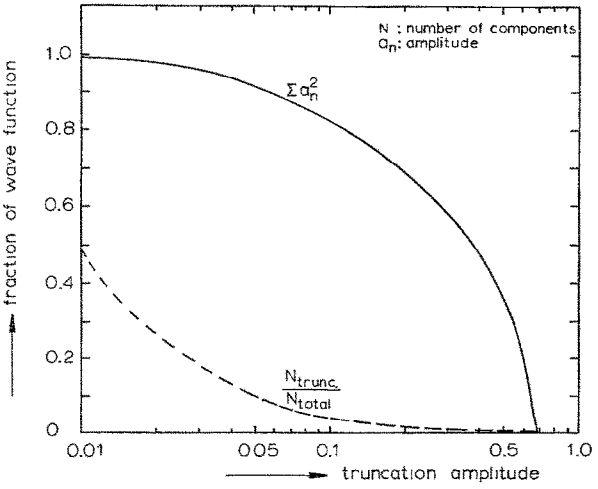

Fig. 1. The number of components of the truncated wave functions and the fraction of the total wave function versus the smallest amplitude taken into account. The two quantities plotted represent an average for the wave functions used for the transitions indicated in fig. 2. The fraction of the total wave function is defined as $\Sigma_{n=1}^{N} a_n^2$ where a_n represents the amplitude of the nth wave function component and N the number of components taken into account.

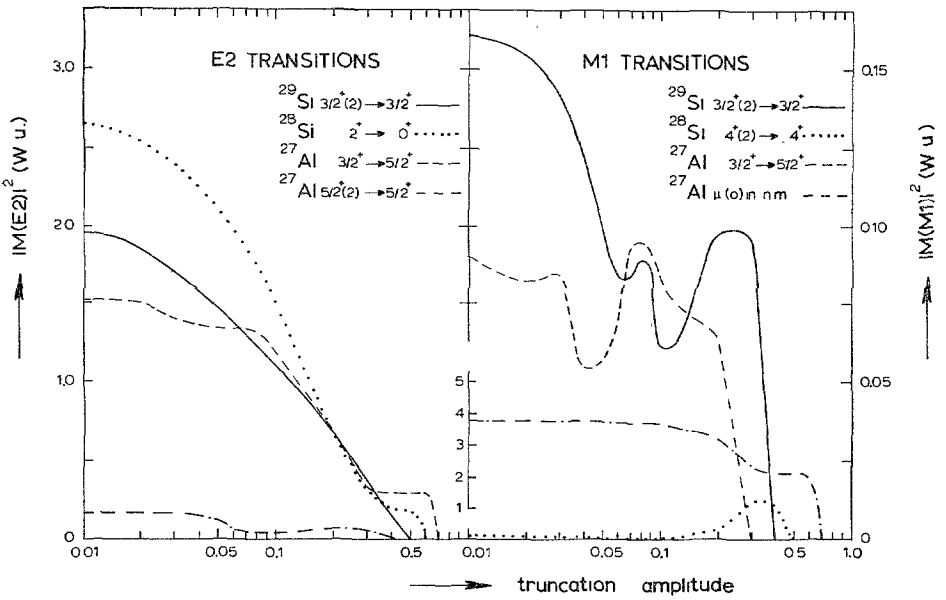

Fig. 2. The influence of amplitude truncation on the calculated E2 and M1 transition strengths. Given are typical examples of transitions in $A = 27$, 28 and 29 nuclei and of one dipole moment. The strengths differ from those given in table 1 since bare-nucleon g-factors and charges are used here.

the fitting procedure, are assumed to be equal to the signs calculated from the wave functions with bare-nucleon g-factors and charges [8]). The experimental errors Δ have been used in the calculations with the following restrictions:

(i) $\Delta \geqq 0.01$ and 0.5 W.u. for M1 and E2 transitions, respectively;

(ii) $\Delta \geqq 25\,\%$ and $10\,\%$ for M1 and E2 transitions, respectively, between the lowest states of given spin and parity;

(iii) $\Delta \geqq 50\,\%$ for all other transitions;

(iv) $\Delta \geqq 5\,\%$ and $25\,\%$ for the magnetic dipole and electric quadrupole moments, respectively.

The arguments for applying these restrictions are discussed in ref. [8]). The second restriction also reflects the fact that the present wave functions reproduce E2 transition strengths much better than M1 strengths.

It was found that most transitions from the $E_x = 4.51$ MeV, $J^\pi = \frac{11}{2}^+$ level and the $E_x > 4.8$ MeV levels in ^{27}Al as well as those from the second $J^\pi = 0^+$ and 3^+ levels in ^{28}Si could not be reproduced. Therefore these transitions have been omitted from later fitting procedures reported below.

3. Results

3.1. ELECTRIC QUADRUPOLE TRANSITIONS AND MOMENTS

Good fits to the experimental data of 72 E2 transition strengths and two quadrupole moments have been obtained with different procedures. First only one effective

TABLE 1

Measured [and calculated] E2 and M1 transition strengths in A = 27-29 nuclei [a]

$E_i \rightarrow E_f$ (MeV)	$\|M(E2)\|^2$(W.u.)	$\|M(M1)\|^2(10^{-2}$W.u.)	$E_i \rightarrow E_f$ (MeV)	$\|M(E2)\|^2$(W.u.)	$\|M(M1)\|^2(10^{-2}$W.u.)
^{27}Al			^{27}Si		
0.84 → 0	8.8 ± 0.6 [7.3]		0.78 → 0	11.5 ± 1.4[9.2]	
1.01 → 0	9.1 ± 1.9 [8.3]	1.3 ± 0.2 [2.4]	0.96 → 0	7.2 ± 1.7[10]	1.70 ± 0.18[1.8]
1.01 → 0.84	[5.8]	8.3 ± 1.4 [4.8]	0.96 → 0.78	[3.4]	<9.0 [5.4]
2.21 → 0	11 ± 3 [4]	6.0 ± 0.6 [5.3]	2.16 → 0	8 ± 3 [10]	5.1 ± 0.7 [4.6]
2.73 → 0	0.15 ± 0.11[1.6]	2.6 ± 0.8 [0.6]	2.65 → 0	1.3 ± 0.8[3.6]	1.1 ± 0.5 0.18]
2.73 → 0.84	<4.9 [4.4]		2.65 → 0.78	9 ± 5 [3.6]	
2.73 → 1.01	7 ± 3 [4.5]	33 ± 10 [51]	2.65 → 0.96	2 ± 2 [2.5]	20 ± 8 [45]
2.98 → 0	<0.03 [0.5]	20.8 ± 1.5 [15]	2.87 → 0	[0.84]	[9.7]
3.00 → 0	7.4 ± 0.7 [5.0]		2.91 → 0	9.6 ± 1.2[8.9]	
3.00 → 2.21	<0.3 [0.14]	6.6 ± 1.6 [16]	2.91 → 2.16	[1.0]	<7.0 [13]
4.51 → 2.21	6.4 ± 0.7 [0.67]		^{28}Si		
4.51 → 3.00	3.4 ± 0.9 [0.46]	0.43 ± 0.08[0.11]	1.78 → 0	13.2 ± 0.5[13]	
4.58 → 0	0.18 ± 0.09[0.13]	1.2 ± 0.4 [7.3]	4.62 → 1.78	14.7 ± 1.3[17]	
4.58 → 1.01	<1.0 [1.5]		4.98 → 1.78	12 ± 3 [0.84]	
4.58 → 2.21	<0.06 [0.10]	2.4 ± 0.8 [0.20]	6.28 → 1.78	<0.01 [0.001]	0.03 ± 0.01[0.08]
			6.28 → 4.62	<1.1 [0.79]	<0.1 [0.02]
			6.89 → 1.78	0.7 ± 0.2[0.52]	
^{27}Mg			6.89 → 4.62	<4.4 [0.89]	<0.5 [0.10]
0.99 → 0	5.9 ± 1.6 [9.7]	2.2 ± 0.5 [3.8]	7.38 → 0	0.32± 0.12[1.1]	
1.70 → 0	9.8 ± 1.6 [9.2]		7.38 → 1.78	<2.3 [2.5]	<1.5 [0.04]
1.94 → 0	1.8 ± 0.4 [0.15]		8.33 → 0		<0.02 [0.03]
1.94 → 0.99	<0.9 [0.3]	2.2 ± 0.4 [3.8]	8.33 → 1.78	<0.03 [0.04]	<0.03 [0.03]
3.11 → 0.99	3.1 ± 1.7 [3.6]		8.54 → 4.62	2.9 ± 0.6[2.5]	
^{29}Si			^{29}P		
1.27 → 0	5.1 ± 1.5 [5.9]	3.9 ± 0.4 [5.5]	1.38 → 0	4 ± 2 [7.0]	5.8 ± 0.7 [7.2]
2.03 → 0	9.8 ± 1.4 [8.8]		1.95 → 0	15 ± 2 [7.6]	
2.03 → 1.27	[1.1]	<1.0 [0.07]	1.95 → 1.38	[0.6]	4.0 ± 1.2 [0.004]
2.43 → 0	9 ± 4 [4.9]	8 ± 2 [6.3]	2.42 → 0	1.6 ± 0.5[2.2]	4.4 ± 0.9 [10]
2.43 → 1.27	<9.0 [8.7]	13 ± 5 [9.6]	2.42 → 1.38	[7.9]	8 ± 2 [10]
3.07 → 1.27	13 ± 8 [7.2]	19 ± 6 [2.8]	3.11 → 1.38	7 ± 4 [7.8]	13 ± 4 [2.5]
3.07 → 2.03	[0.17]	[7.3]	3.11 → 1.95	<13 [1.2]	17 ± 6 [11]
4.08 → 1.27	10.4 ± 1.7 [6.8]		4.08 → 1.38	34 ± 8 [8.6]	
4.08 → 2.03	0.40 ± 0.16[3.2]	2.9 ± 0.5 [1.1]	4.08 → 1.95	2.3 ± 1.5[5.0]	13 ± 3 [1.4]
4.74 → 2.03	21 ± 5 [11]				
^{29}Al					
1.40 → 0	8 ± 5 [2.6]				

[a] Experimental strengths are taken from ref. [14]; see also for ^{27}Mg refs. [15-17]), ^{27}Al refs. [18-21]), ^{27}Si refs. [22-24]), ^{28}Si refs. [25-27]), ^{29}Al refs. [28-30]), ^{29}Si refs. [31-34]) and for ^{29}P refs. [35-37]). Experimental information taken from references not mentioned explicitly, will be compiled in the forthcoming edition of ref. [14]). Calculated strengths are given in square brackets. For spins see figs. 3–7.

TABLE 2

Calculated E2 and M1 strengths of transitions from analogue states in $A = 27$ and 29 nuclei [a])

	^{27}Al–^{27}Si			^{29}Si–^{29}P	
J_i, T_i [b]) $\rightarrow J_f, T_f$	$\lvert M(\mathrm{E2})\rvert^2$ (W.u.)	$\lvert M(\mathrm{M1})\rvert^2$ (10^{-2}W.u.)	J_i, T_i [b]) $\rightarrow J_f, T_f$	$\lvert M(\mathrm{E2})\rvert^2$ (W.u.)	$\lvert M(\mathrm{M1})\rvert^2$ (10^{-2}W.u.)
$\frac{1}{2}, \frac{3}{2} \rightarrow \frac{5}{2}, \frac{1}{2}$	0.3		$\frac{5}{2}, \frac{3}{2} \rightarrow \frac{1}{2}, \frac{1}{2}$	0.2	
$\frac{1}{2}, \frac{1}{2}$		0.06	$\frac{3}{2}, \frac{1}{2}$	0.005	17
$\frac{3}{2}, \frac{1}{2}$	0.07	53	$\frac{5}{2}, \frac{1}{2}$	0.2	17
$\frac{3}{2}, \frac{3}{2} \rightarrow \frac{5}{2}, \frac{1}{2}$	0.07	2.3	$\frac{1}{2}, \frac{3}{2} \rightarrow \frac{1}{2}, \frac{1}{2}$		9.4
$\frac{1}{2}, \frac{1}{2}$	0.09	15	$\frac{3}{2}, \frac{1}{2}$	0.07	4.6
$\frac{3}{2}, \frac{1}{2}$	0.03	0.3	$\frac{5}{2}, \frac{1}{2}$	0.04	

[a]) Given are only the transitions from the lowest two analogue states to the lowest three $T = \frac{1}{2}$ states.

[b]) The excitation energies of the $J^\pi = \frac{1}{2}^+$ and $\frac{3}{2}^+$ analogue states in $A = 27$ and of the $J^\pi = \frac{5}{2}^+$ and $\frac{1}{2}^+$ states in $A = 29$ are calculated [9]) as $E_x = 6.32$, 7.78, 8.29 and 9.60 MeV, respectively.

charge parameter $e_p + e_n$ was determined while the charge difference was fixed at the bare-nucleon value $e_p - e_n = e$. A second fit with separate effective charges for protons and neutrons did not improve the results significantly. Finally, an independent adjustment of the three most important isoscalar reduced single-particle matrix elements, involving the transitions $d_{\frac{5}{2}} \leftrightarrow d_{\frac{5}{2}}$, $s_{\frac{1}{2}} \leftrightarrow d_{\frac{5}{2}}$ and $d_{\frac{3}{2}} \leftrightarrow s_{\frac{1}{2}}$, did not provide much better agreement between calculated and measured transition strengths than the first, one-parameter fit mentioned above. Therefore the final results, given in tables 1 and 2, are those obtained with effective charges determined in the one-parameter fit.

From the least-squares fit one finds for the effective proton and neutron charges $e_p = 1.60e$ and $e_n = 0.60e$, respectively. From similar calculations in the mass region $A = 30$–34, values of $e_p = 1.44e$ and $e_n = 0.68e$ [ref. [8])] were obtained. These values do not deviate much from the effective charges $e_p = 1.5e$ and $e_n = 0.5e$, commonly assumed in shell-model calculations for light nuclei [see e.g. refs. [10,38])].

The average absolute deviation between experiment and theory for the E2 transitions given in table 1 is 3.0 W.u., while the average measured strength of these transitions is 7.7 W.u. The calculated electric quadrupole moments agree excellently with the experimental data, given in figs. 4 and 5.

3.2. MAGNETIC DIPOLE TRANSITIONS AND MOMENTS

Results for calculated M1 transition rates which represent improvements over the use of bare-nucleon single-particle matrix elements could only be obtained by treating the $A = 27$ and 29 nuclei separately. The explanation given for a similar effect in the mass region $A = 30$–34 [ref. [8])] is also valid in the present case, namely that the M1 transitions, which have a pronounced single-particle character (see subsect. 4.2), are much more affected by the closure of the $1d_{\frac{5}{2}}$ subshell than are the more collective E2 transitions. Another important reason might be the configuration space used, which for $A = 29$ is somewhat different from that for $A = 27$ and 28 (see sect. 1).

TABLE 3

Comparison between bare-nucleon and effective reduced single-particle M1 matrix elements (in n.m.)

$\langle l_f j_f \|\|M1\|\| l_i j_i \rangle$ [a])	Bare-nucleon value	$A = 27$–29 [b])	$A = 27$ [c])		$A = 29$ [d])	
$\langle d_{\frac{5}{2}} \|\|M1\|\| d_{\frac{5}{2}} \rangle_s$	2.88	2.8±0.4				
$\langle s_{\frac{1}{2}} \|\|M1\|\| s_{\frac{1}{2}} \rangle_s$	0.75	0.8±0.2				
$\langle d_{\frac{3}{2}} \|\|M1\|\| d_{\frac{3}{2}} \rangle_s$	1.14	2.6±0.4				
$\langle d_{\frac{5}{2}} \|\|M1\|\| d_{\frac{3}{2}} \rangle_s$	−0.41	−0.4±0.2				
$\langle s_{\frac{1}{2}} \|\|M1\|\| d_{\frac{3}{2}} \rangle_s$	0	0.2±0.1				
$\langle d_{\frac{5}{2}} \|\|M1\|\| d_{\frac{5}{2}} \rangle_v$	11.63	8.9±0.3	10.3±0.8		8.1±0.7	9.1±0.6
$\langle s_{\frac{1}{2}} \|\|M1\|\| s_{\frac{1}{2}} \rangle_v$	6.90	4.2±0.3	4.1±0.6	4.3±0.6	5.7±0.6	
$\langle d_{\frac{3}{2}} \|\|M1\|\| d_{\frac{3}{2}} \rangle_v$	−1.58	−3.1±0.6	−4 ±7		1.9±1.0	
$\langle d_{\frac{5}{2}} \|\|M1\|\| d_{\frac{3}{2}} \rangle_v$	−7.80	−4.2±0.5	−12.8±1.6	−13.8±0.9	−4.3±1.0	
$\langle s_{\frac{1}{2}} \|\|M1\|\| d_{\frac{3}{2}} \rangle_v$	0	1.0±0.2	−0.7±0.9		1.8±0.2	1.0±0.2

[a]) The indices s and v label the isoscalar and isovector parts, respectively.

[b]) Determined from a least-squares fit to 48 observed transition strengths and three dipole moments in the mass region $A = 27$–29.

[c]) Determined from five- and two-parameter fits to 16 M1 strengths and one dipole moment. The matrix elements not given are kept at the bare-nucleon values.

[d]) Determined from five- and two-parameter fits to 19 M1 strengths and two dipole moments. For matrix elements not given see footnote [c]).

Fits to 16 (19) M1 transitions with measured strengths larger than 0.01 W.u. and one (two) magnetic dipole moment(s) for $A = 27$ (29) were obtained first by adjusting the four effective g-factors and later with two effective isovector reduced single-particle matrix elements (r.s.p.m.e.) as variable parameters, while the remainder was kept constant at the bare-nucleon values. The final results, given in tables 1 and 2, are taken from the latter fit because of the smaller number of free parameters and the better possibilities for physical interpretation. The values for the r.s.p.m.e., calculated from the bare-nucleon g-factors and the effective values obtained from the least-squares fits are given in table 3. It is remarkable that the values of the ten effective r.s.p.m.e., given in column 3 of table 3, which are obtained from a separate fit to 51 experimental data in the complete mass region $A = 27$–29 are very close to the bare-nucleon values.

It was possible to diminish the number of free parameters by fixing poorly determined matrix elements at the bare-nucleon values. In this way five- and two-parameter fits (see table 3) have been performed without spoiling the agreement with experiment. The agreement between calculated and measured magnetic dipole moments, given in figs. 4 and 7, is good except for the ^{27}Al ground state, although the bare-nucleon value (3.74 n.m.) in this case is close to the measured value (3.64 n.m.).

The average absolute deviation between experiment and theory for the M1 transitions given in table 1 is 0.05 W.u., while the average strength of these transitions is 0.08 W.u.

3.3. OBSERVABLE QUANTITIES

Lifetimes, branching and mixing ratios, calculated from the transition strengths given in table 1 are compared with experimental data in figs. 3–7. The excitation energies are discussed in ref. [9]).

The signs of the calculated mixing ratios follow from the relative signs of the E2 and M1 amplitudes. The phase convention of Rose and Brink [39]) is used throughout. The agreement between calculated and experimentally determined mixing ratios is very good, especially for transitions from low-lying levels. The calculations are in line with the rule [40]) that mixing ratios for corresponding transitions in mirror nuclei have about equal absolute values and opposite signs. The only significant exception is the pair of mixing ratios calculated for the transitions between the lowest $J^\pi = \frac{5}{2}^+$ and $\frac{3}{2}^+$ levels in ^{29}Si and ^{29}P (see fig. 7). The large mixing ratios in ^{28}Si (see fig. 5) reflect

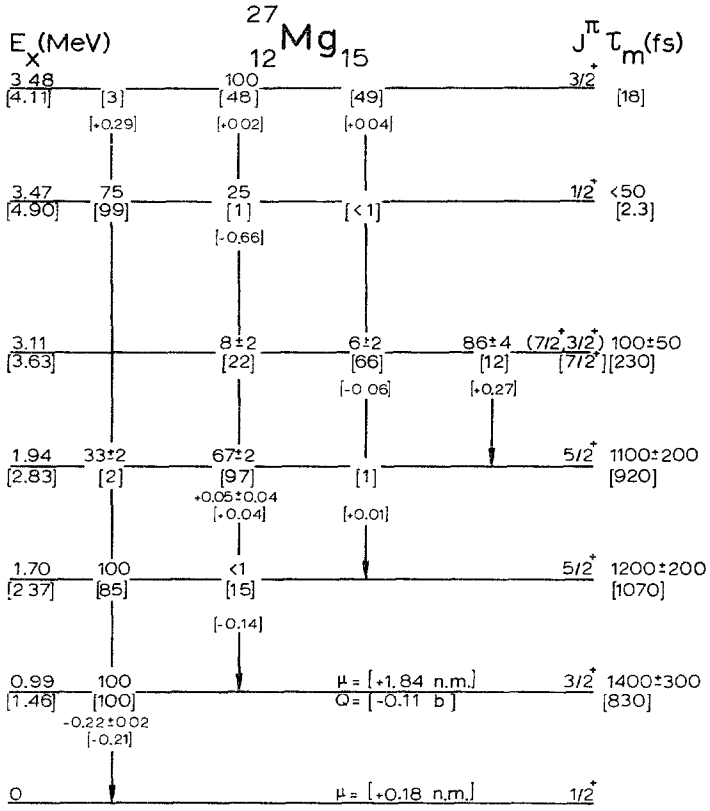

Fig. 3. Comparison between calculated [in square brackets] and measured quantities for ^{27}Mg. The experimental data have been taken from refs. [14–17]). The lowest two levels of each spin are given if sufficient experimental information is available. The excitation energies are given in a distorted scale; the calculated energies are from ref. [9]). Extra spacing between two levels indicates omission of experimentally known (even parity) levels. The signs of the mixing ratios are all given in the phase convention of Rose and Brink [39]).

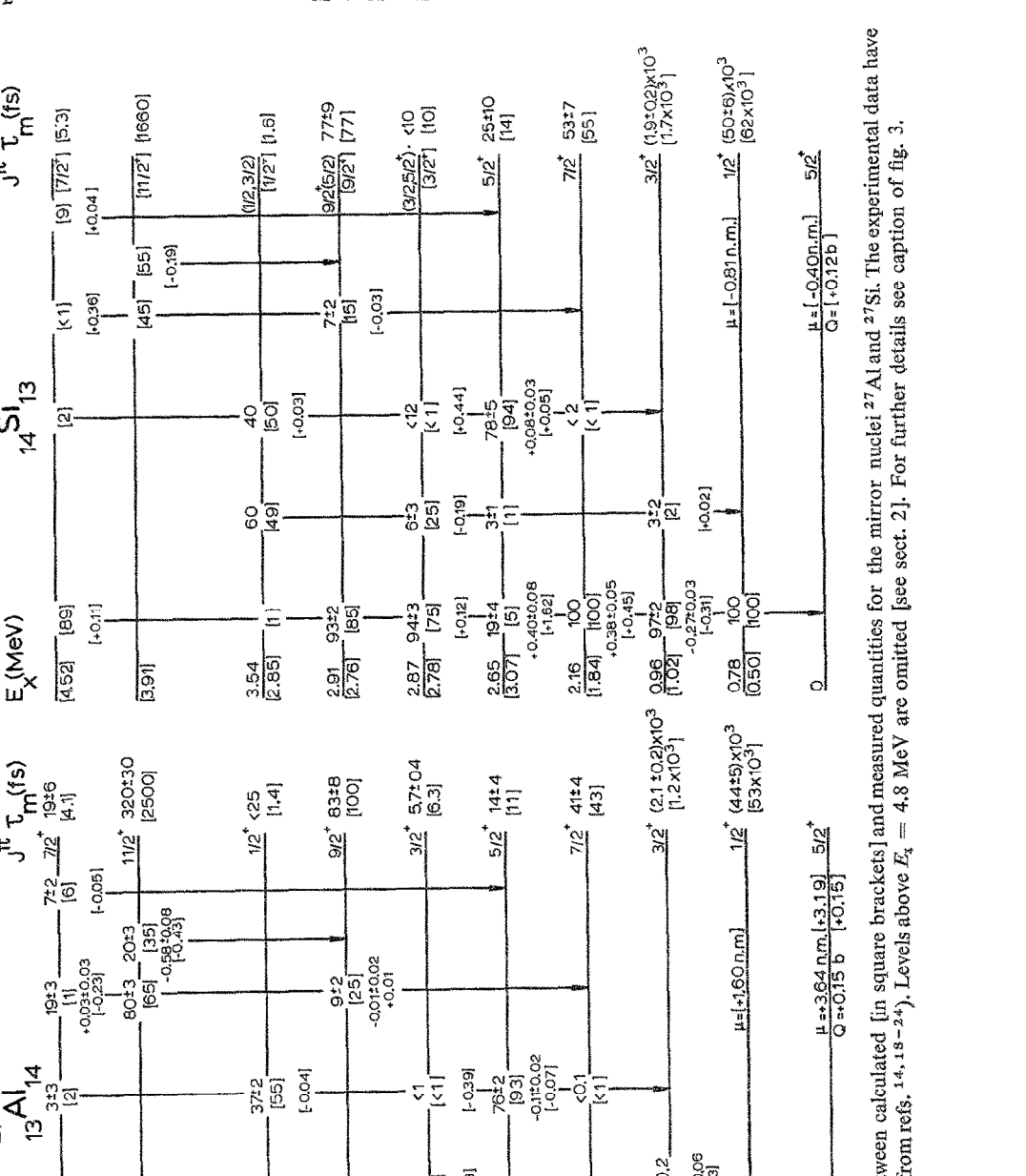

Fig. 4. Comparison between calculated [in square brackets] and measured quantities for the mirror nuclei ^{27}Al and ^{27}Si. The experimental data have been taken from refs. [14,18–24]). Levels above $E_x = 4.8$ MeV are omitted [see sect. 2]. For further details see caption of fig. 3.

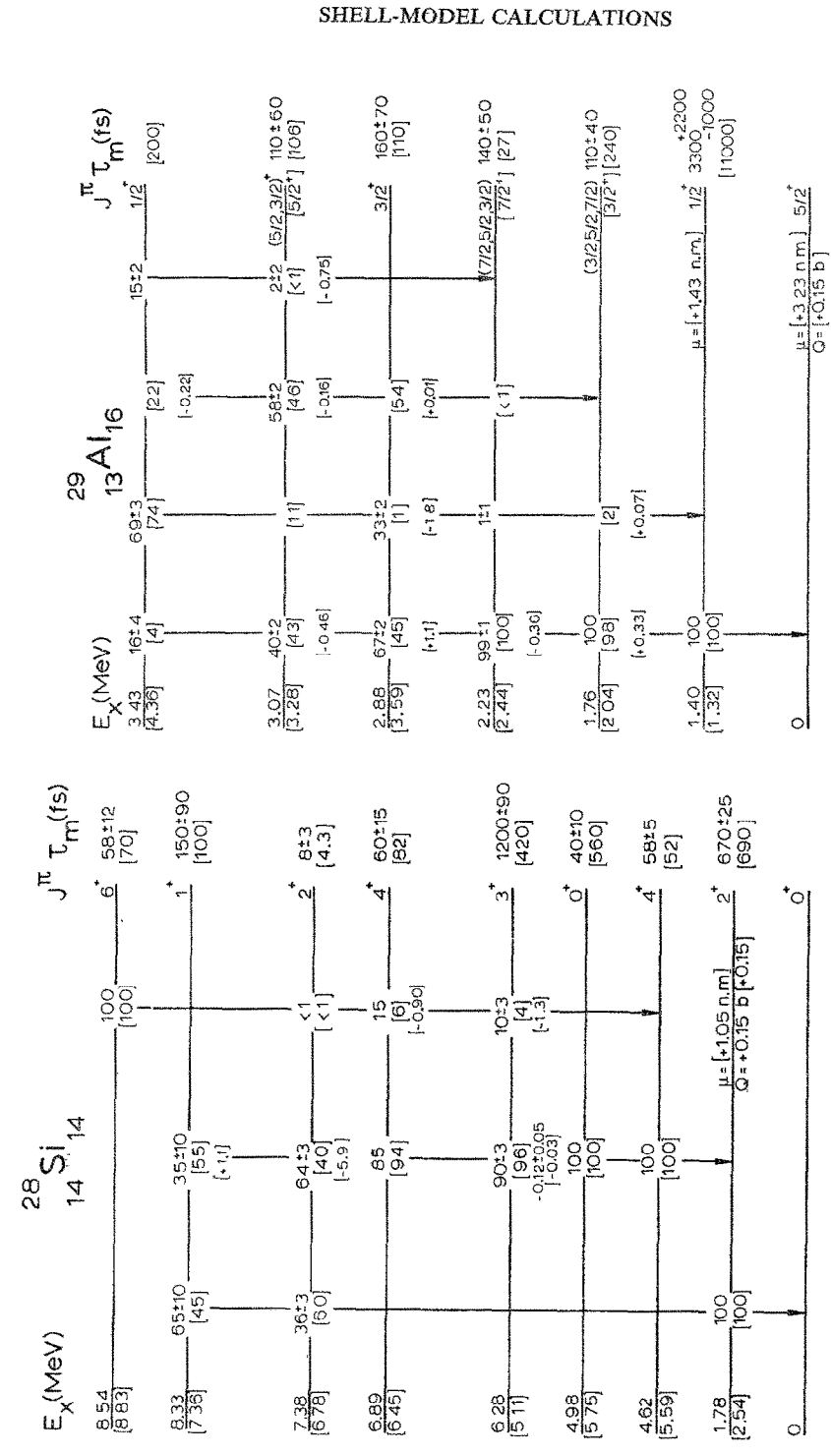

Fig. 5. Comparison between calculated [in square brackets] and measured quantities for ^{28}Si. The experimental data have been taken from refs. [14,25–27]). The second $J^\pi = 3^+$ level is omitted [see sect. 2]. For further details see caption of fig. 3.

Fig. 6. Comparison between calculated [in square brackets] and measured quantities for ^{29}Al. The experimental data have been taken from refs. [14,28,29]) and in particular the lifetimes of the second and higher levels from ref. [30]). For further details see caption of fig 3.

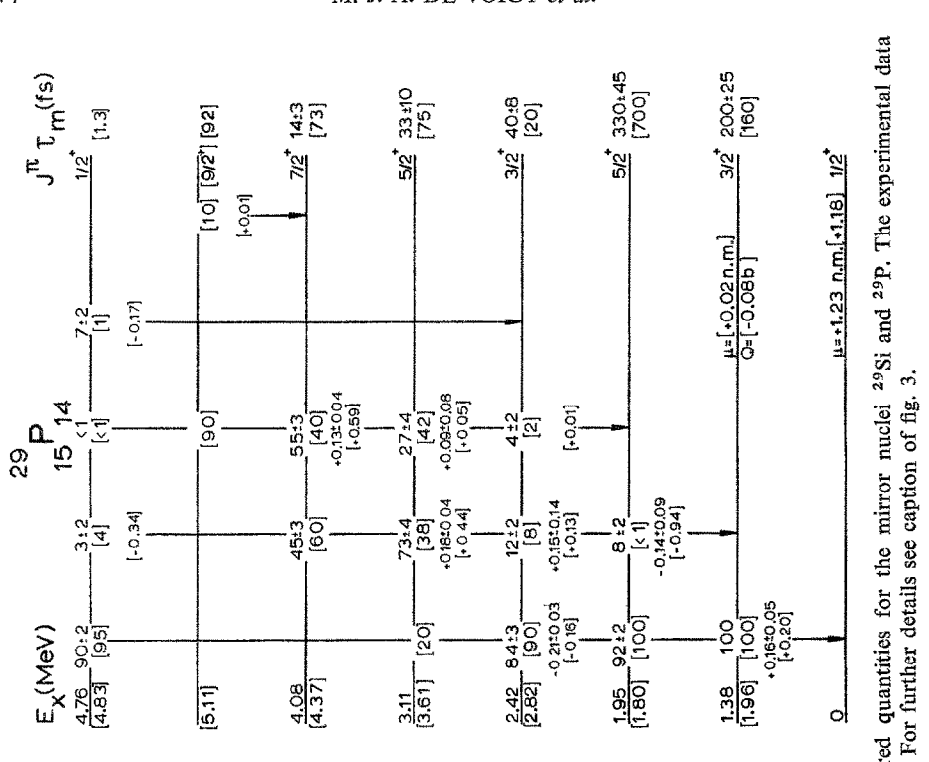

Fig. 7. Comparison between calculated [in square brackets] and measured quantities for the mirror nuclei ^{29}Si and ^{29}P. The experimental data have been taken from refs. [14,31–37]). For further details see caption of fig. 3.

TABLE 4
Comparison between experimental and theoretical log ft values

Transition	$J_i, T_i \to J_f, T_f$	Exp. [a])	Theory
$^{27}Si \to {}^{27}Al$	$\frac{5}{2}, \frac{1}{2} \to \frac{5}{2}, \frac{1}{2}$	3.55±0.05	3.53
	$\frac{3}{2}, \frac{1}{2}$	6.80±0.15	5.24
	$\frac{7}{2}, \frac{1}{2}$	4.94±0.09	5.12
	$\frac{5}{2}(2), \frac{1}{2}$	5.09±0.06	5.19
	$\frac{3}{2}(2), \frac{1}{2}$	4.51±0.09	4.72
$^{27}Mg \to {}^{27}Al$	$\frac{1}{2}, \frac{3}{2} \to \frac{1}{2}, \frac{1}{2}$	4.6 ±0.2	4.19
	$\frac{3}{2}, \frac{1}{2}$	5.3 ±0.2	4.42
$^{29}P \to {}^{29}Si$	$\frac{1}{2}, \frac{1}{2} \to \frac{1}{2}, \frac{1}{2}$	3.72±0.05	3.66
	$\frac{3}{2}, \frac{1}{2}$	4.84±0.07	4.72
	$\frac{3}{2}(2), \frac{1}{2}$	4.24±0.11	4.13
$^{29}Al \to {}^{29}Si$	$\frac{5}{2}, \frac{3}{2} \to \frac{3}{2}, \frac{1}{2}$	5.09±0.01	4.53
	$\frac{5}{2}, \frac{1}{2}$	5.74±0.05	4.85
	$\frac{3}{2}(2), \frac{1}{2}$	4.99±0.05	4.40
	$\frac{5}{2}(2), \frac{1}{2}$	6.16±0.18	4.89

[a]) Refs. [14, 43–48]).

the strong hindrance [41]) of $\Delta T = 0$ M1 transitions in self-conjugated nuclei. The fact that the mixing ratio in ^{28}Si for the transition between the lowest $J^\pi = 3^+$ and 2^+ levels is small, is due to the very small E2 strength. Comparison of the experimental mixing ratios in ^{27}Si and ^{27}Al for the $\frac{5}{2}^+(2) \to \frac{5}{2}^+(1)$ transition is difficult [24]), because of the uncertainties in the latter for which conflicting values have been published [14, 21, 42]).

Calculated log ft values are compared with experimental data in table 4. It was not meaningful to perform a separate least-squares fit for the β-transitions, because of the scarceness of experimental data. Therefore effective Gamow-Teller matrix elements for β-decay have been calculated from the effective M1 matrix elements given in table 3, by means of a procedure discussed in ref. [8]). The log ft values calculated with these effective Gamow-Teller matrix elements do not agree significantly better with experiment than those obtained with the bare-nucleon values. For β^+ transitions between mirror nuclei the agreement with experiment is acceptable except for the $^{27}Si(\frac{5}{2}^+) \to {}^{27}Al(\frac{3}{2}^+)$ transition, whereas all calculated log ft values for $\Delta T = 1$, β^- transitions are significantly smaller than the measured values (see table 4). The difficulties to reproduce observed log ft values and M1 transitions in the present model (see subsect. 4.2) are probably related, due to the similarity of the corresponding operators.

4. Discussion

4.1. SUMMARY OF THE RESULTS

Adjustment of a single parameter (the isoscalar effective charge) suffices to produce electric quadrupole transition strengths and moments calculated from shell-model

wave functions, which agree very well with the experimental data for $A = 27$–29. Slightly worse, but still generally acceptable, agreement with experiment results from calculating magnetic dipole transition strengths and moments based on an M1 operator for which two reduced single-particle matrix elements are adjusted to obtain a best fit to the experimental strengths for $A = 27$ and 29 separately, while the remainder is kept constant to the bare-nucleon values. The present model does not reproduce the properties of the $E_x = 4.51$ MeV, $J^\pi = \frac{1}{2}^+$ level and the $E_x > 4.8$ MeV levels in ^{27}Al, and those of the second $J^\pi = 0^+$ and 3^+ states in ^{28}Si.

The isoscalar part of the E2 operator and the isovector part of the M1 operator are the most important parts [see also ref. [8])]. Therefore only the corresponding parameters were varied in the final fitting procedures. The very small E2 strengths given in table 2 derive from the fact that the isoscalar part vanishes for $\Delta T = 1$ transitions.

The necessity to treat the M1 transitions for $A = 27$ and 29 nuclei separately is clearly demonstrated by the very different corrections to the bare-nucleon reduced single-particle matrix elements (see table 3). One finds that the present wave functions do not correctly take into account $s_{\frac{1}{2}} \leftrightarrow s_{\frac{1}{2}}$ and $d_{\frac{3}{2}} \leftrightarrow d_{\frac{3}{2}}$ contributions to M1 transitions for $A = 27$ and $d_{\frac{5}{2}} \leftrightarrow d_{\frac{5}{2}}$ and $d_{\frac{3}{2}} \leftrightarrow s_{\frac{1}{2}}$ contributions for $A = 29$. The most important contributions to M1 transition strengths follow from the $d_{\frac{5}{2}} \leftrightarrow d_{\frac{5}{2}}$ and $d_{\frac{3}{2}} \leftrightarrow d_{\frac{5}{2}}$ single-particle transitions for $A = 27$ and from the $s_{\frac{1}{2}} \leftrightarrow s_{\frac{1}{2}}$ and $d_{\frac{3}{2}} \leftrightarrow d_{\frac{3}{2}}$ transitions for $A = 29$.

4.2. THE CHARACTER OF E2 AND M1 TRANSITIONS

The collective behaviour of E2 transitions is demonstrated by the smooth curves in fig. 2, indicating the constructive interference of many small wave function components. Therefore in a more extended configuration space one will obtain larger E2 strengths. The single-particle character of M1 transitions is demonstrated by the strongly fluctuating curves in fig. 2, which indicate constructive and sometimes destructive interference of a few large components. A more extended configuration space will therefore not necessarily imply larger M1 strengths. This capricious character makes it difficult to fit M1 strengths to experimental data, when they are calculated from truncated wave functions.

It is also clear from fig. 2 that the calculation of transition strengths from the stronger wave function components only, e.g. with amplitudes larger than 0.1 as given in ref. [49]), may lead to considerable errors.

4.3. COMPARISON WITH OTHER MODELS

The transition strengths and multipole moments from the present calculation for ^{27}Al can be compared to those of rotation-vibration [1]) and excited-core [2]) model calculations. In general the three different model calculations reproduce the experimental facts equally well. The properties of the $E_x = 1.01$ MeV, $J^\pi = \frac{3}{2}^+$ level, however, are better reproduced in the present calculation.

For ^{28}Si, Hartree-Fock (HF) calculations [3, 4]) lead to somewhat better agreement

with experimental excitation energies of low-lying levels than the present model [9]). However, the best agreement with experiment for these levels is obtained from shell-model calculations employing a combination of realistic and empirically determined two-body matrix elements [50]). The E2 strengths for transitions within the ground-state rotational band in ^{28}Si from the present and the HF calculations [3, 4]) agree equally well with experiment. For the $J^\pi = 6^+ \rightarrow 4^+$ transition in this band, HF calculations lead to E2 strengths of 15.5 W.u. [Das Gupta and Harvey as quoted in ref. [52])] and 6.9 W.u. [ref. [4])] and the present calculation of 2.5 W.u. In this respect the lifetime of the $E_x = 8.54$ MeV, $J^\pi = 6^+$ level plays a crucial role. There are two measured lifetimes reported, leading to two conflicting experimental strengths for this transition, of 2.9 ± 0.6 and 9.4 ± 3.0 W.u. The lifetime $\tau_m = 58 \pm 12$ fs deduced from a DSA ^{25}Mg(α, nγ) experiment [51]) at $E_\alpha = 7$ MeV is to be preferred over the $\tau_m = 18 \pm 6$ fs value from a DSA ^{27}Al(p, γ) experiment [52]) at $E_p = 2.2$ MeV on the basis of possible stopping-power problems [19]) in the latter.

The excitation energies of the low-lying ^{29}Si levels are much better reproduced by the modified intermediate-coupling model (ICM) [ref. [5])] than by the present calculation [9]). The present M1 strengths for transitions in ^{29}Si are comparable to ICM results if in the latter case two-particle one-hole contributions [53]) are taken into account.

It should be mentioned that in the present shell-model calculations the level schemes follow from fits to experimental data in the complete mass region $A = 27$–29 with only four free parameters. In collective model treatments the level schemes, transition rates and multiple moments in general follow from fits to the experimental data in one specific nucleus, involving at least six free parameters, which is about a factor of three more per nucleus than in the present calculation.

It is a pleasure to thank Prof. P. M. Endt and Dr. C. van der Leun for their continuous interest and for valuable discussions and J. van Hienen for assistance with computer programs.

This work was performed as part of the research programme of the Stichting voor Fundamenteel Onderzoek der Materie (FOM) with financial support from the Nederlandse Organisatie voor Zuiver-Wetenschappelijk Onderzoek (ZWO).

References

1) H. Röpke, V. Glattes and G. Hammel, Nucl. Phys. **A156** (1970) 477
2) D. Evers, J. Hertel, T. W. Retz-Schmidt and S. J. Skorka, Nucl. Phys. **A91** (1967) 472
3) S. Das Gupta and M. Harvey, Nucl. Phys. **A94** (1967) 602
4) B. Castel and J. C. Parikh, Phys. Rev. **C1** (1970) 990
5) B. Castel, K. W. C. Stewart and M. Harvey, Can. J. Phys. **48** (1970) 1490
6) R. G. Hirko, thesis, Yale University, 1969
7) B. H. Wildenthal, J. B. McGrory, E. C. Halbert and P. W. M. Glaudemans, Phys. Lett. **27B** (1968) 611
8) P. W. M. Glaudemans, P. M. Endt and A. E. L. Dieperink, Ann. of Phys. **63** (1971) 134

9) B. H. Wildenthal and J. B. McGrory, to be published
10) B. H. Wildenthal, J. B. McGrory and P. W. M. Glaudemans, Phys. Rev. Lett. **26** (1971) 96
11) J. van Hienen, Utrecht, private communication, 1971
12) J. B. French, E. C. Halbert, J. B. McGrory and S. S. M. Wong, in Adv. in Nucl. Phys. ed.; M. Baranger and E. Vogt, vol. 3 (Plenum New York, 1969)
13) P. W. M. Glaudemans, P. J. Brussaard and B. H. Wildenthal, Nucl. Phys. **A102** (1967) 593
14) P. M. Endt and C. van der Leun, Nucl. Phys. **A105** (1967) 1 and to be published
15) G. Costa and F. A. Beck, Nucl. Phys. **A181** (1972) 132
16) D. H. Sykes *et al.*, Nucl. Phys. **A135** (1969) 335
17) L. C. McIntyre, P. L. Carson and D. L. Barker, Phys. Rev. **184** (1969) 1105
18) M. J. A. de Voigt, J. W. Maas, D. Veenhof and C. van der Leun, Nucl. Phys. **A170** (1971) 449
19) M. J. A. de Voigt, J. Grootenhuis, J. B. van Meurs and C. van der Leun, Nucl. Phys. **A170** (1971) 467
20) P. J. M. Smulders, C. Broude and J. F. Sharpey-Schafer, Can. J. Phys. **46** (1968) 261
21) A. H. Lumpkin *et al.*, Phys. Rev. **C4** (1971) 1215
22) I. Mauritzson, R. Engmann, F. Brandolini and V. Barci, Nucl. Phys. **A174** (1971) 572
23) J. J. Weaver *et al.*, Nucl. Phys. **A172** (1971) 577
24) I. G. Main *et al.*, J. of Phys. **A4** (1971) L59
25) M. A. Meyer, N. S. Wolmarans and D. Reitmann, Nucl. Phys. **A144** (1970) 261
26) I. Forsblom, Comm. Phys. Math. **40** (1970) 65
27) F. C. P. Huang, E. F. Gibson and D. K. McDaniels, Phys. Rev. **C3** (1971) 1222
28) A. D. W. Jones, J. A. Becker and R. E. McDonald, Phys. Rev. **187** (1969) 1388
29) A. D. W. Jones, J. A. Becker and R. E. McDonald, Phys. Rev. **C3** (1971) 724
30) G. Costa and F. A. Beck, Strasbourg, private communication, 1972
31) G. Main *et al.*, Nucl. Phys. **A158** (1970) 364
32) T. T. Bardin, J. A. Becker, T. R. Fisher and A. D. W. Jones, Phys. Rev. **C4** (1971) 1625
33) A. A. Pilt, R. H. Spear, R. V. Elliott and J. A. Kuehner, Can. J. Phys. **49** (1971) 1263
34) J. S. Forster, C. Broude and W. G. Davies, Nucl. Phys. **A161** (1971) 375
35) F. A. Beck, Strasbourg, private communication, 1971
36) R. P. Williams, S. G. Buccino and C. C. Wellborn, Nucl. Phys. **A151** (1970) 504
37) C. F. Monahan *et al.*, Can. J. Phys. **48** (1970) 2683
38) M. R. Gunye, Phys. Lett. **37B** (1971) 125
39) H. J. Rose and D. M. Brink, Revs. Mod. Phys. **39** (1967) 306
40) P. W. M. Glaudemans and C. van der Leun, Phys. Lett. **34B** (1971) 41
41) E. K. Warburton and J. Weneser, Isospin in nuclear physics, ed. D. H. Wilkinson (North-Holland, Amsterdam, 1969) p. 185
42) T. R. Ophel and B. T. Lawergren, Nucl. Phys. **52** (1964) 417
43) D. Berenyi, D. A. Hutcheon, D. F. H. Start and J. J. Weaver, Nucl. Phys. **A178** (1971) 76
44) C. Détraz, C. E. Moss and C. S. Zaidins, Phys. Lett. **34B** (1971) 128
45) R. A. Bigoni, S. D. Bloom and K. G. Tirsell, Nucl. Phys. **A134** (1969) 620
46) T. T. Bardin and J. A. Becker, Phys. Rev. Lett. **27** (1971) 866
47) W. R. Harris, K. Nagatani and D. E. Alburger, Phys. Rev. **187** (1969) 1445
48) F. M. Mann and R. W. Kavanagh, Bull. Am. Phys. Soc. **17** (1972) 90
49) B. H. Wildenthal, J. B. McGrory, E. C. Halbert and H. D. Graber, Phys. Rev. **C4** (1971) 1708
50) J. B. McGrory and B. H. Wildenthal, Phys. Lett. **34B** (1971) 373
51) S. T. Lam, A. E. Litherland and T. K. Alexander, Can. J. Phys. **47** (1969) 1371
52) F. C. P. Huang and D. K. McDaniels, Phys. Rev. **C2** (1970) 1342
53) B. Castel and I. P. Johnstone, Can. J. Phys. **49** (1971) 1641